nature publishing group

TLR2 promotes macrophage recruitment and *Streptococcus pneumoniae* clearance during mouse otitis media

Yifei Huang[1,2], Zimeng Wang[1], Chunfang Jin[1], Lei Wang[1], Xuemei Zhang[1], Wenchun Xu[1], Yun Xiang[1], Wei Wang[1], Xiujing He[2], Yibing Yin[1] and Yujuan He[1]

BACKGROUND: The natural course of otitis media (OM) in most children is acute and self-limiting; however, approximately 10–20% of children can experience persistent or recurrent OM. Determining the host factors that influence outcome of OM will help us design better therapies. This study focused on the role of Toll-like receptor 2 (TLR2) in a pneumococcal OM mouse model.

METHODS: The middle ears (MEs) of wild-type (WT) and TLR2$^{-/-}$ mice were inoculated with *Streptococcus pneumoniae* (*Spn*) serotype 19F via transbullar injection. ME TLR2 expression in WT mice was determined by qRT-PCR and immunofluorescence. ME pathological manifestations, inflammatory response, and pneumococcal clearance between WT and TLR2$^{-/-}$ mice were compared after *Spn* inoculation.

RESULTS: TLR2 expression in ME mucosa was markedly enhanced following infection with *Spn* in WT mice. In contrast to WT mice, TLR2$^{-/-}$ mice exhibited unaffected early ME inflammatory response. During late stage of ME infection, however, the absence of TLR2 can lead to reduced macrophage recruitment, impaired *Spn* clearance, and prolonged ME inflammation.

CONCLUSION: Our results demonstrate that TLR2 signaling is critical for bacterial clearance and timely resolution of inflammation in OM induced by *Spn*.

Otitis media (OM) is one of the most common pediatric infectious disease, and 50 to 80% of children have had OM at least once by age of 3 y in developed country (1,2). The natural course of OM in most children is acute and self-limiting (3). Approximately 10 to 20% of children, however, can experience recurrent or persistent OM and resultantly suffer long-term hearing loss due to scarring of the ME conductive apparatus or sensorineural damage to the inner ear (4,5). *Streptococcus pneumoniae* (*Spn*), one of the most common pathogens associated with OM, is responsible for 19 to 74% of total episodes (6,7). Antibiotic use is, up till now, the major treatment of OM (8). However, the increasing pneumococcal resistance and the emergence of multiple resistant *Spn* have led to a review of the antibiotic treatment of children with OM (1,9–11). Therefore, it is urgent to explore alternative therapies based on new insights into the pathophysiology of OM (3).

As the best characterized class of pattern recognition receptor family, Toll-like receptors (TLRs) recognize the pathogen-associated molecular patterns of invading bacteria and regulate the production of cytokines and chemokines that orchestrate the recruitment of neutrophils and macrophages to clear invading bacteria at the site of infection (12,13). Clinical studies have revealed that the deficiency of IRAK-4 and MyD88, which are important adapter proteins of TLRs signaling pathway, was associated with a selective predisposition to pneumococcal infections in children (14–16). Furthermore, the susceptibility of pneumococcal sepsis and meningitis in MyD88$^{-/-}$ mice were significantly increased (17,18). These findings suggest TLRs signaling pathway plays an important role in host defense against pneumococcal infections. Among the defined 10 members of human TLRs, the Toll-like receptor 2 (TLR2), which locates in the plasma membrane of mucosal epithelial cells and innate immune cells, is activated by pneumococcal cell wall components, such as lipoteichoic acid and lipoproteins (19), has been proved to induce inflammatory response and enhance pneumococcal phagocytosis and intracellular killing in leucocytes (20). During pneumococcal pneumonia, TLR2$^{-/-}$ mice exhibited slightly reduced levels of proinflammatory cytokines and unaffected *Spn* clearance (21). In a model of pneumococcal meningitis, however, TLR2$^{-/-}$ mice showed significantly reduced early leucocyte influx and impaired *Spn* clearance, as well as higher susceptibility to aggravated disease progression (22). These paradoxical results indicate that the role of TLR2 in pneumococcal infections depends on distinct tissue microenvironment (23).

To date, an *in vitro* research has revealed that pneumococcal peptidoglycan-polysaccharides can activate TLR2 expression in mouse ME epithelial cells through NF-κB signaling pathway (24). The TLR2 mRNA expression in ME effusion of children with OM also increased (25). More importantly, genetic

The first two authors contributed equally to this work.
[1]Key Laboratory of Diagnostic Medicine Designated by the Ministry of Education, Chongqing Medical University, Chongqing, China; [2]Department of Laboratory Medicine, Reproductive and Genetic Hospital of CITIC-Xiangya, Changsha, China. Correspondence: Yujuan He (100951@cqmu.edu.cn)

Received 16 March 2016; accepted 10 June 2016; advance online publication 5 October 2016. doi:10.1038/pr.2016.154

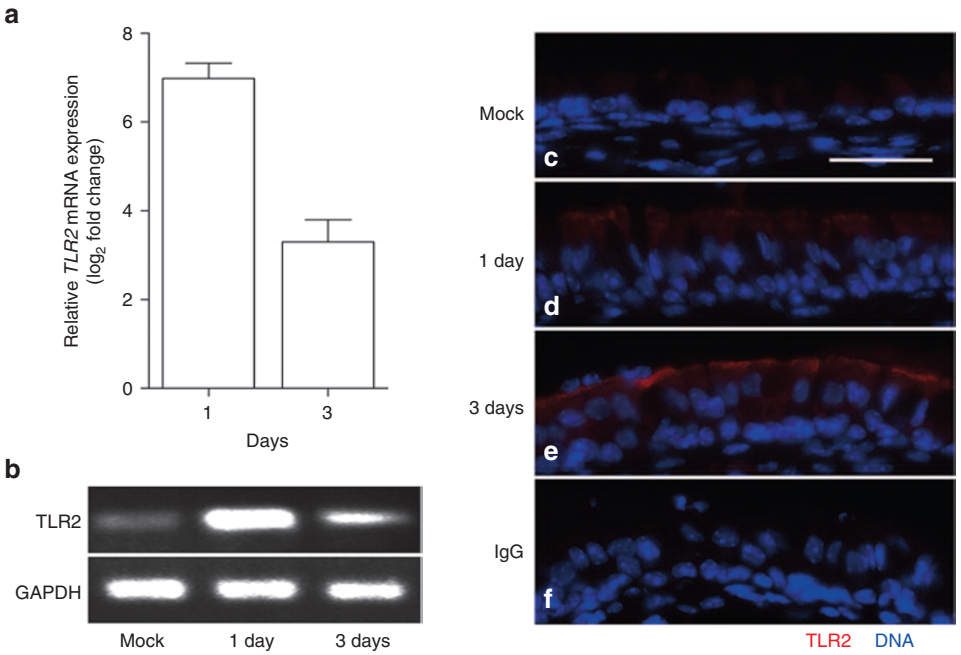

Figure 1. Expression of ME TLR2 during pneumococcal OM. ME TLR2 mRNA expression were determined using qRT-PCR (**a**) and semi-quantitative PCR (**b**) at 1 and 3 d after *Spn* infection. Mock: PBS-treated ME. Data are combined from three independent experiments with at least six mice in each group. Values are expressed relative to PBS-treated group and represent mean $\log_2 \pm$ SD. ME TLR2 protein expression were determined using immunofluorescence at 1 d (**c**) and 3 d (**d**) after *Spn* infection. Mock: PBS-treated ME (**e**). IgG: nonspecific stain control for the upper row TLR2 stain (**f**). Red represents TLR2 protein and blue for cell nucleus. Scale bar = 50 µm. Original magnification: ×40.

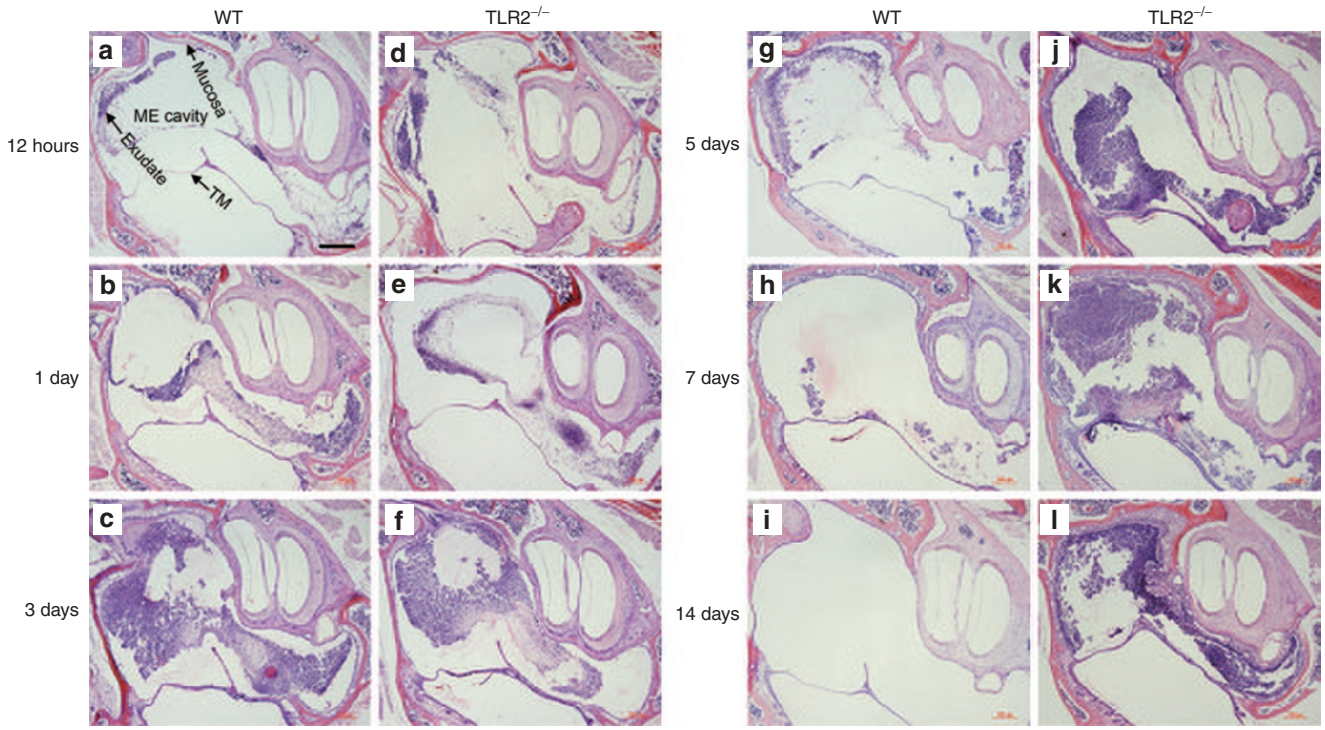

Figure 2. ME histology during pneumococcal OM. Twelve hours (**a**), 1 d (**b**), 3 d (**c**), 5 d (**g**), 7 d (**h**), 14 d (**i**) after *Spn* inoculation in WT mice. Twelve hours (**d**), 1 d (**e**), 3 d (**f**), 5 d (**j**), 7 d (**k**), 14 d (**l**) after *Spn* inoculation in $TLR2^{-/-}$ mice. In WT mice, an exudate with inflammatory cells was noted in the ME cavity from 12 h (**a**), and this change reached the most prominent at 3 d (**c**). Thereafter, the exudate became to weaken from 5 d (**g**) and almost disappeared at 14 d (**i**). $TLR2^{-/-}$ mice exhibited similar pathological changes with WT mice from 12 h to 3 d (**d–f**). However, at 5 to14 d after *Spn* infection, the MEs of $TLR2^{-/-}$ mice showed a persistent inflammatory cell infiltration and ME mucous thickening compared with WT mice (**j–l**). ME, middle ear; TM, tympanic membrane. Scale bar = 500 µm. Original magnification: ×4.

polymorphisms in TLRs and its downstream signal molecules, like TNFα, IL-6 and IL-10, have been proved to be associated with the recurrence and persistence of OM (26,27). Taken together, we inferred that TLR2 likely plays an important role in the pathogenesis of pneumococcal OM.

To investigate the role of TLR2 in pneumococcal OM, we established a mouse model of OM induced by *Spn* and compared the dynamics of ME pathologic change, inflammatory response and bacterial clearance between WT and TLR2$^{-/-}$ mice.

RESULTS

ME TLR2 Expression Is Upregulated During Pneumococcal OM

Using qRT-PCR, we found that TLR2 mRNA was constitutively expressed in healthy ME and markedly enhanced following infection with pneumococci (**Figure 1a**,**b**). Compared with PBS controls, *Spn*-infected mice were found to be nearly 100-fold upregulated in terms of TLR2 mRNA at 1 d and 8-fold at 3 d after *Spn* infection, respectively (**Figure 1b**). Using immunofluorecence, we found that TLR2 protein expression in the surface epithelium of ME was also increased gradually and became evident at 3 d (**Figure 1c–f**), which was correlated with TLR2 mRNA expression.

ME Pathological Changes in TLR2$^{-/-}$ Mice Are Persistent After *Spn* Infection

To investigate the role of TLR2 in pathogenesis of OM, we compared the ME response to *Spn* in WT mice and TLR2$^{-/-}$ mice. As depicted in **Figure 2a–f**, exudate with inflammatory cells began to appear within 12 h and nearly filled up the entire ME cavity of WT and TLR2$^{-/-}$ mice at 3 d after *Spn* inoculation. In WT mice, the exudate decreased gradually from 5 d and almost disappeared at 14 d (**Figure 2g–i**). During this period, however, the ME cavity of TLR2$^{-/-}$ mice was still filled with considerable inflammatory cells and exudate, accompanied by the obvious pathological manifestations of tympanic membrane and ME mucosa (**Figure 2j–l**). By comparing the pathological changes of ME mucosa near the eustachian tube orifice between WT and TLR2$^{-/-}$ mice, we found that both of them exhibited similar inflammatory performance like vasodilation and leukocytic infiltration and mucosal hyperplasia in the early stage of *Spn* infection (12 h to 3 d, **Figure 3a–f** and **Figure 3m**). Mucosal thickness in this site of WT mice began to decrease from 5 d, indicating the recovery of mucosal inflammation (**Figure 3g–i** and **Figure 3m**). However, the vasodilation and leukocytic infiltration failed to recover in TLR2$^{-/-}$ mice (**Figure 3j–l**), and mucosal thickness was significantly greater than that of the WT mice (**Figure 3m**).

Resolution of ME Inflammation in TLR2$^{-/-}$ Mice Is Delayed After *Spn* Infection

To further confirm these above findings, we acquired and analyzed the middle ear lavage fluid (MELF) of WT mice and TLR2$^{-/-}$ mice at different time points after *Spn* inoculation. The number of inflammatory cells and the level of proinflammatory cytokines like TNF-α, IL-6, and IL-1β in MELF of TLR2$^{-/-}$ mice were both higher than WT mice in the late stage of ME

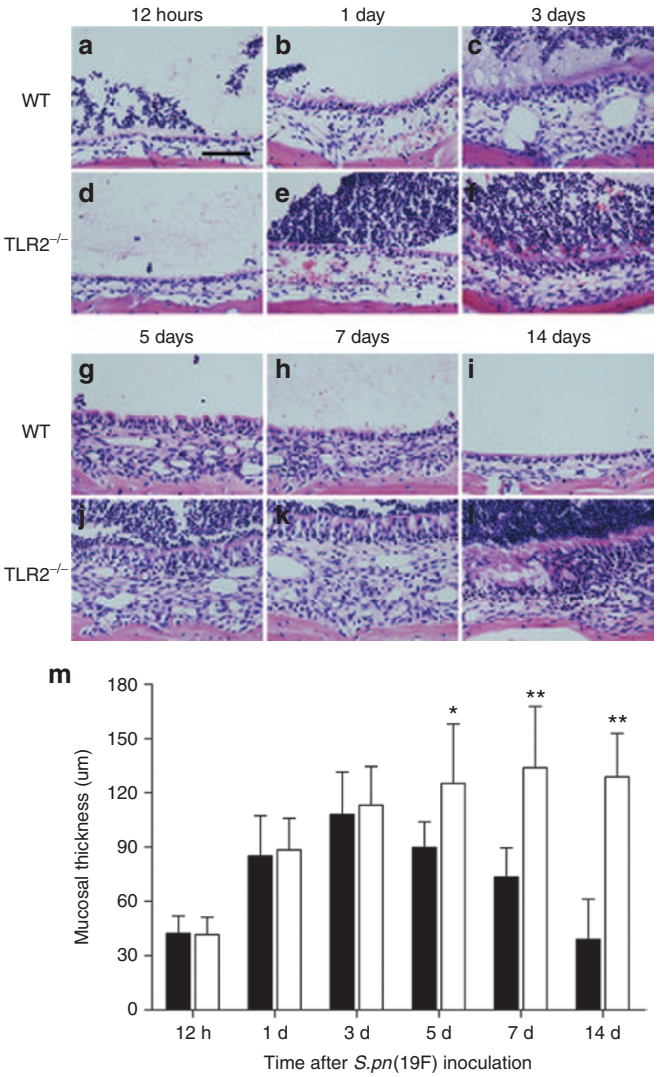

Figure 3. Dynamics of pathologic change in ME mucosa. Representative hemotoxylin and eosin staining of ME mucosa from WT and TLR2$^{-/-}$ mice. Twelve hours (**a**), 1 d (**b**), 3 d (**c**), 5 d (**g**), 7 d (**h**), 14 d (**i**) after *Spn* inoculation in WT mice. Twelve hours (**d**), 1 d (**e**), 3 d (**f**), 5 d (**j**), 7 d (**k**), 14 d (**l**) after *Spn* inoculation in TLR2$^{-/-}$ mice. (**m**) ME mucosal thickness of WT and TLR2$^{-/-}$ mice at different time point after *Spn* inoculation. Black fill columns, WT mice; no fill columns, TLR2$^{-/-}$ mice. $n = 16$ ears per group per time point. $^{*}P < 0.05$ and $^{**}P < 0.01$ vs. WT mice. Values represent means ± SD. Scale bar = 100 μm. Original magnification: ×20.

infection (5 and 7 d, **Figure 4a**,**b**), which is correlated with the result of histopathology (**Figure 2**) and indicates the prolonged ME inflammation in TLR2$^{-/-}$ mice. In the early stage, however, no similar significant differences between WT and TLR2$^{-/-}$group were observed (**Figure 4a**,**c**). Taken together, these results indicate that deficiency of TLR2 signal delays the recovery of pneumococcal OM, but have little effect during the early initiation phase of ME inflammation.

TLR2 Contributes to *Spn* Clearance in ME Cavity

MELF was used to evaluate the kinetics of ME infection by quantitative culture. The density of *Spn* in MELF of WT mice decreased gradually over the observation period and almost

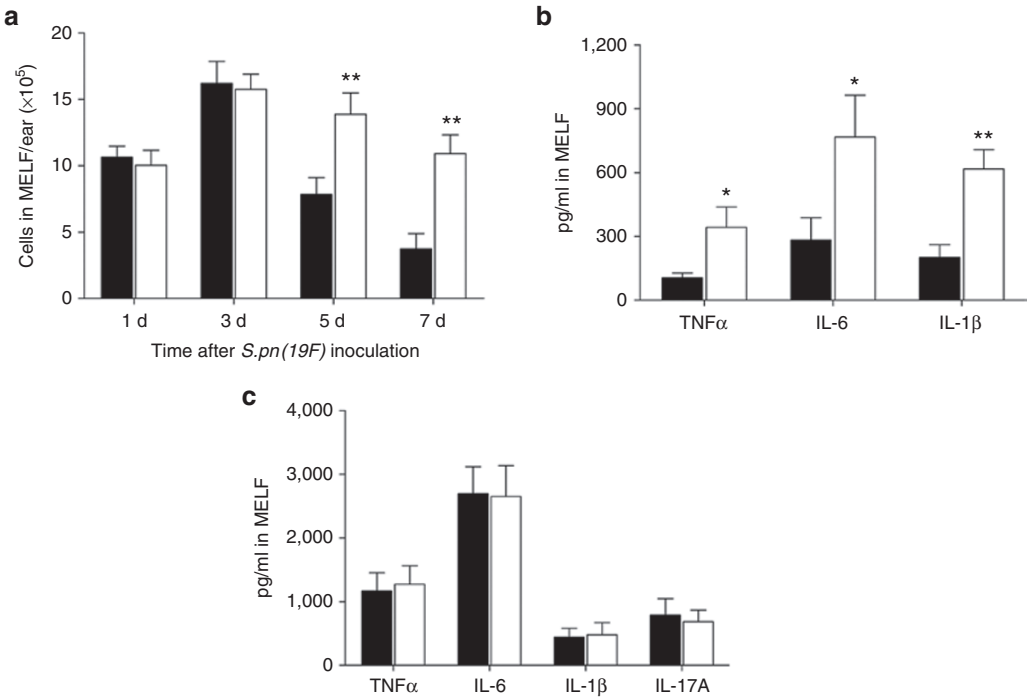

Figure 4. Persisted ME inflammation in TLR2$^{-/-}$ mice. (**a**) Amount of infiltrating inflammatory cells in the MELF of WT and TLR2$^{-/-}$ mice at the time indicated following *Spn* inoculation. (**b**) TNF-α, IL-6, and IL-1β levels in the MELF of WT and TLR2$^{-/-}$ mice at 7 d after *Spn* inoculation. (**c**) TNF-α, IL-6, IL-1β, and IL-17A levels in the MELF of WT and TLR2$^{-/-}$ mice at 1 d after *Spn* inoculation. Black fill columns, WT mice; no fill columns, TLR2$^{-/-}$ mice. $n = 16$ ears per group per time point. *$P < 0.05$ and **$P < 0.01$ vs. WT mice. Values represent means ± SD.

fell below the limit of detection (13/16 ears) at 7 d after inoculation (Figure 5a). In contrast, *Spn* in MELF of TLR2$^{-/-}$ mice were steadily recovered and significantly outnumbered that of WT group during the late stage of OM (5 and 7 d, Figure 5a). Immunofluorescence staining of MELF cytospin preparations showed that many intact pneumococci located in ME cavity of TLR2$^{-/-}$ mice at 5 and 7 d, while only small amount of pneumococcal debris was observed in WT mice (Figure 5b), which is consistent with bacterial quantitative culture. Meanwhile, with the clearance of *Spn*, the inflammatory cells in WT mice showed significant degeneration and consequently few survived with intact morphology, which was different from TLR2$^{-/-}$ mice. These findings suggest that TLR2 deficiency impairs the ability of *Spn* clearance and leads to a persistent ME inflammation.

Macrophage Recruitment Is Reduced in ME Cavity of TLR2$^{-/-}$ Mice

Neutrophils and macrophages have been confirmed as important host effector cells to clear *Spn* at the site of infection. At 1 d after *Spn* inoculation, the majority of ME inflammatory cells in WT and TLR2$^{-/-}$ mice were neutrophils (over 95%, CD11b^{+}Ly6G^{+}), macrophages (CD45^{+}F4/80^{+}) accounted only for 2%. At 3 d, the percentage of macrophages in WT mice rose to 7 to 9%, whereas it remained 2 to 4% in TLR2$^{-/-}$ mice (Figure 6a,c); Parallelly, the macrophages in WT mice also out numbered those in TLR2$^{-/-}$ mice at 3 d, except for the neutrophils (Figure 6b). Consistently, our histopathology results showed that less macrophages were observed in the ME cavity of TLR2$^{-/-}$ mice than WT mice at 3 d (Figure 6d).

DISCUSSION

The heterogeneity of ME infection's outcome among different children is a long-standing clinical challenge, but the mechanism underlying this phenomenon is still unclear. In this study, we established a mouse model of pneumococcal OM via transbullar injection and found that TLR2 expression in WT mice ME was markedly upregulated. In contrast to WT mice, TLR2$^{-/-}$ mice showed a prolonged ME inflammation and persistent ME pathological changes (leukocytic infiltration in ME cavity and ME mucosal hyperplasia) at the late stage of pneumococcal OM, which correlated with the impaired pneumococcal clearance in ME cavity. We also found that macrophage recruitment of TLR2$^{-/-}$ mice was significantly reduced during ME pneumococcal infection.

It has been documented that different pattern recognition receptors play important roles in host defense against pneumococcal infection of different organs. In early research, we evaluated mRNA expression profile of TLR2, TLR4, TLR9, NOD2, and NLRP3, which were involved in recognition of *Spn* (23), in ME after *Spn* challenge (unpublished data). We found that upregulation of TLR2 mRNA, not others, was the most significant. We also confirmed an increased expression of TLR2 protein in ME mucosa by immunofluorescence, which is consistent with the finding of pneumococcal peptidoglycan-polysaccharides stimulating ME epithelial cells in vitro (24). Using a mouse OM model induced by *Spn* serotype 6A via transtympanic injection, Han *et al.* found that over 60% TLR2$^{-/-}$ mice died within 3 d after inoculation (28), which was different from local infection characteristics of human OM (3).

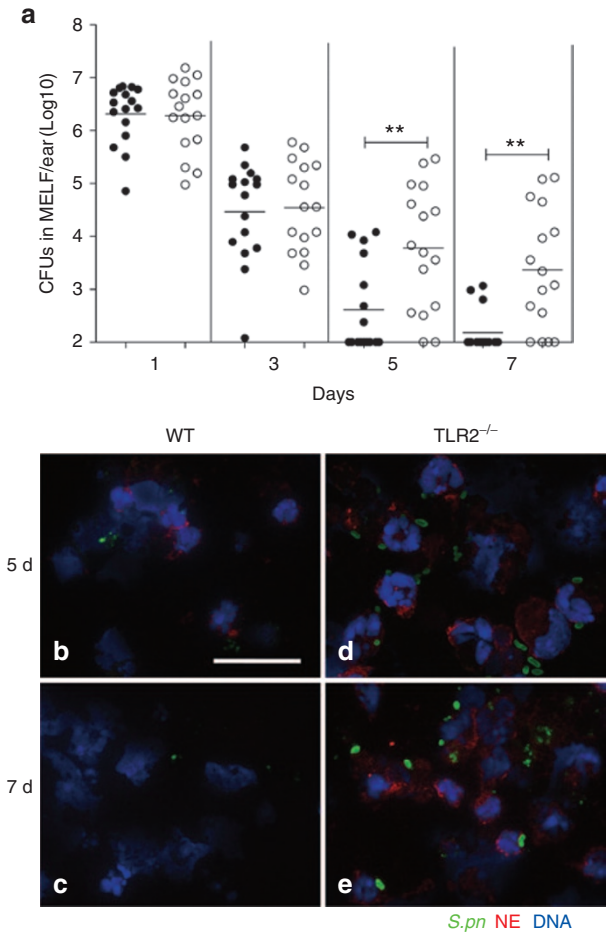

Figure 5. Impaired *Spn* clearance in ME cavity of TLR2$^{-/-}$ mice. (**a**) Pneumococcal load in the MELF of WT and TLR2$^{-/-}$ mice at the time indicated following *Spn* inoculation. Black fill symbols, WT mice; no fill symbols, TLR2$^{-/-}$ mice. Horizontal lines indicate mean values. One dot represents one ear. $n = 16$ ears per group per time point. $^{**}P < 0.01$ vs. WT mice. (**b**) Representative immunofluorescence staining of MELF cytospin preparations from WT (left panel) and TLR2$^{-/-}$ mice (right panel) at 5 and 7 d after *Spn* inoculation. Green represents *Spn*; red represents neutrophil elastase (NE, a maker for neutrophil), and blue for cell nucleus. Pneumococci were observed in TLR2$^{-/-}$ mice but not WT mice at 5 and 7 d. Scale bar = 25 μm. Original magnification: ×40.

In this study, TLR2$^{-/-}$ mice exhibited impaired *Spn* clearance as well as continuous ME inflammation, suggesting an indispensable role of TLR2 signaling for the resolution of OM, albeit no death occurred in the entire observation period. The apparent discrepancy may be explained by the following reasons: first, pneumococcal strain used in our study was the clinical isolate 31693 (serotype 19F, which is most frequently serotype isolated from OM patients and proved to be noninvasive (29)) with a dose of 5×10^4 CFUs per ear, much less than Han's 1×10^6 CFUs per ear. Second, we adopted transbullar injection method to induce OM in the mouse model, which is under a direct view and can reduce the damage to cochlea significantly (30).

We found no significant difference in the quantity of inflammatory cells and the levels of proinflammatory cytokines like TNF-α, IL-6, and IL-1β in MELF between WT and TLR2$^{-/-}$ mice at 1 d post-*Spn* inoculation, suggesting that TLR2 did not play an important role in activating ME inflammatory response during pneumococcal OM. Indeed, several studies have proved that apart from TLR2, other pattern recognition receptors also get involved in recognizing invading *Spn* and leading to production of pro-inflammatory cytokines. For instance, TLR9 detects pneumococcal DNA containing unmethylated CpG motifs within endosomes (31) and lysozyme-digested pneumococcal peptidoglycan fragments are sensed by NOD2 within cytoplasm (32). Our prior studies have demonstrated that IL-17A promotes *Spn* clearance by inducing the recruitment and apoptosis of neutrophils through a p38 MAPK signaling pathway and thus plays an important role in the development of pneumococcal OM (33). In present study, however, there was no significant difference between WT and TLR2$^{-/-}$ mice regarding concentrations of IL-17A in MELF, indicating that TLR2 signaling was not essential for IL-17A production during pneumococcal OM.

Zhang *et al.* previously reported that TLR2$^{-/-}$ mice exhibit prolonged pneumococcal carriage and delayed macrophage recruitment in the nasopharynx, with neutrophil recruitment surprisingly unaffected, indicating a critical role for TLR2-mediated signaling in maintaining macrophage recruitment during pneumococcal colonization (34). Probably the ME cavity and the nasopharynx sharing a substantially similar immunological microenvironment due to the adjacent anatomic location, these findings are consistent with the results in this study. As an important cellular mediator of innate immune defense, macrophage not only have the ability to engulf and kill invading pathogens directly, but also can produce numerous regulatory cytokines or ingest the aged neutrophils to assist a rapid and effective removal of pathogens by other immune effector cells (35,36). Besides, they also can present digested pathogen antigens to the corresponding helper T cell to initiate the adaptive immune response (37). It has been reported that macrophage is essential for defense against *Listeria monocytogenes*, *Mycobacterium* tuberculosis, and *Cryptococcus neoformans* infection in murine model (38). More importantly, in association with the depletion of macrophage with administration of Cl_2MDP liposomes, there was a significantly diminished clearance of *Spn* in the nasopharynx at both 7 and 28 d after inoculation (34). Thus, we hypothesize the impaired *Spn* clearance correlates with reduced macrophage recruitment in TLR2$^{-/-}$ mice.

In summary, our present results demonstrate that TLR2-mediated macrophage recruitment promotes the clearance of *Spn* in ME and thus contributes to the recovery of pneumococcal OM, shedding light on the potential of TLR2 as a novel strategy for OM treatment. However, the molecular mechanism of chemokine expression accounting for the TLR2-mediated macrophage recruitment during pneumococcal OM needs a further clarification.

METHODS

Mice

C57BL/6 mice aged 6–8 wk were obtained from Chongqing Medical University. TLR2$^{-/-}$ mice (B6.129-Tlr2^{tmlKir}/JNju) with C57BL/6 background were purchased from Nanjing Biomedical Research Institute

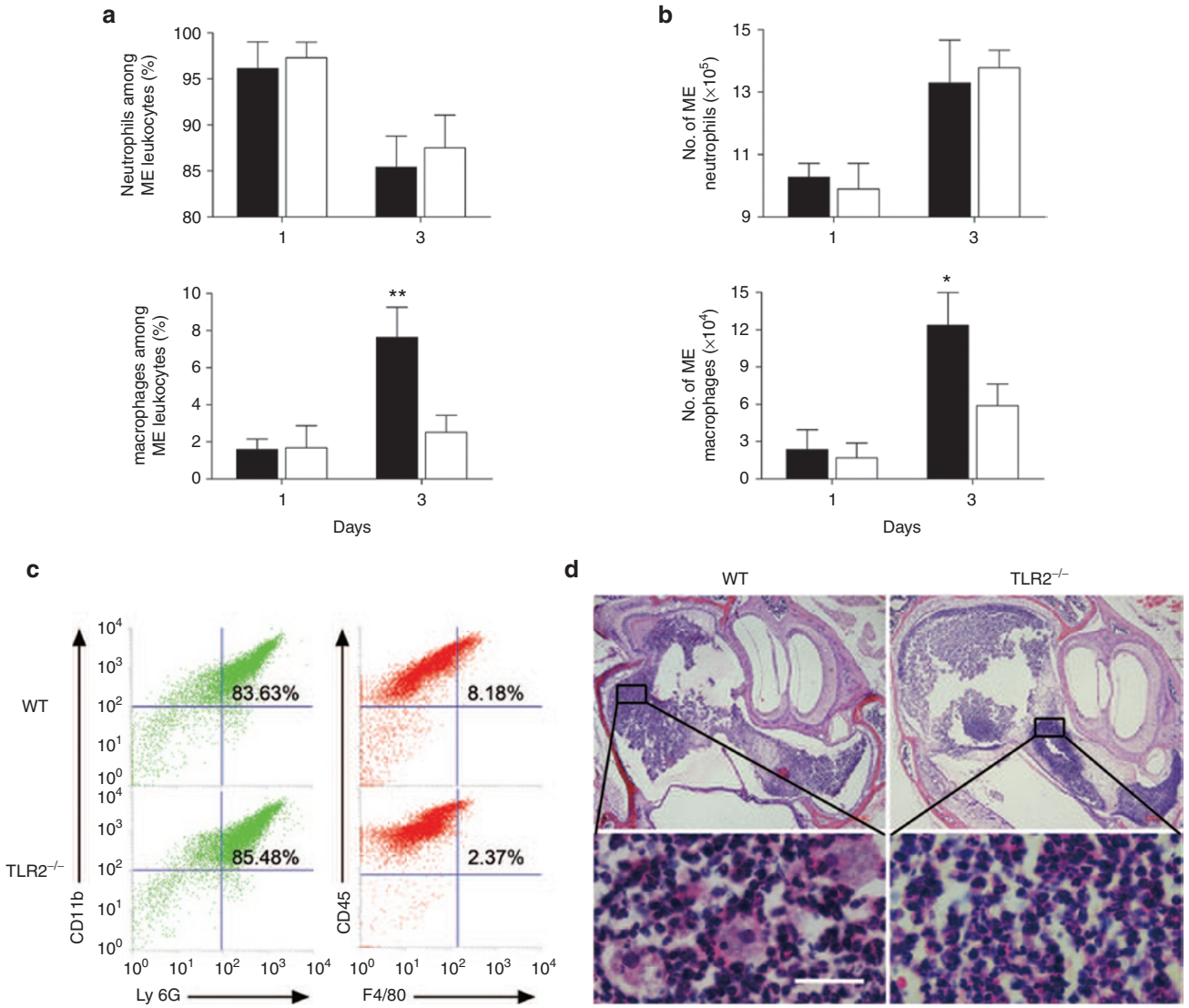

Figure 6. Reduced macrophage not neutrophil recruitment in ME cavity of TLR2$^{-/-}$ mice. Frequency (**a**) and numbers (**b**) of neutrophils and macrophages among the MELF inflammatory cells in WT and TLR2$^{-/-}$ mice at the time indicated following *Spn* inoculation, and determined by flow cytometry. Data are combined from three independent experiments with at least six mice in each group. Black fill columns, WT mice; no fill columns, TLR2$^{-/-}$ mice. *P < 0.05 and **P < 0.01 vs. WT mice. Values represent means ± SD. (**c**) Dot plots showing representative frequencies of neutrophils (CD11b^{+}Ly6G^{+}) and macrophages (CD45^{+}F4/80^{+}) among the MELF inflammatory cells in WT and TLR2$^{-/-}$ mice at 3 d after *Spn* inoculation. (**d**) Representative ME histopathology at 3 d after *Spn* inoculation as shown by hemotoxylin and eosin staining. Scale bar = 50 μm. Original magnification: ×4 (upper panel), ×100 (lower panel).

of Nanjing University. All mice were housed under a specific-pathogen-free environment in the laboratory animal center of Chongqing Medical University. The following experiments were done in accordance with the Institutional Animal Care and Use Committee's guidelines of Chongqing Medical University.

Bacterial Strain

Streptococcus pneumonia clinical isolate 31693 (serotype 19F) was obtained from the National Center for Medical culture Collections (CMCC, Beijing, China) and grown in casein hydrolysate plus yeast extract (C+Y) medium at 37 °C in 5% CO_2 until mid-log phase (OD_{600} = 0.4 to 0.5). After centrifugation, the pneumococcal pellet was washed and resuspended to a density of 1×10^7 CFUs/ml as previously described (33).

Mouse Model of Experimental Otitis Media

The mouse model of OM was established via transbullar injection followed by the method described previously (39,40). In brief, mice were anesthetized with an intraperitoneal injection of ketamine hydrochloride (0.020 mg/g of body weight) and xylazine (0.013 mg/g). Through a ventral midline incision in the neck, the tympanic bulla was exposed bilaterally after blunt dissection. The bony wall of bilateral bulla was fenestrated using a 25-gauge needle and a total of 5×10^4 CFU *Spn* in ~5 μl was injected slowly into the ME cavity with a thinner needle. A mock control cohort of mice was inoculated with an equivalent volume of PBS alone. After that, the skin incision was sutured.

Quantitative Real-Time PCR

The tympanic bullae of WT mice, which encompasses the ME cavity was harvested at indicated time and then spilt longitudinally into dorsal and ventral halves. ME epithelium lining the ME cavity and effusions were lysed and collected with 700 μl RLT lysis buffer from RNeasy mini kit (Qiagen, Valencia, CA). After that, total RNA was isolated from the lysates using the RNeasy mini kit according to manufacturer's protocol (33). cDNA was reverse transcribed using PrimeScript RT reagent Kit with gDNA Eraser (Takara Bio, Kusatsu, Japan). qPCR reactions based on SYBR green detection were performed using SYBR *Premix Ex Taq* II (Takara Bio) on an ABI PRISM 7500 sequence detection system (Applied Biosystems, Foster City, CA), and quantitative comparisons were made using the $\Delta\Delta C_T$

Table 1. Primer sequences for amplification of mouse *TLR2* and *GAPDH*

Gene	Primer sequences
TLR2 (mouse)	Sense primer: 5′-CTCTTCAGCAAACGCTGTTCT-3′
	Anti-sense primer: 5′-GGCGTCTCCCTCTATTGTATTG-3′
GAPDH (mouse)	Sense primer: 5′-AATGGATTTGGACGCATTGGT-3′
	Anti-sense primer:5′-TTTGCACTGGTACGTGTTGAT-3′

method. The reaction protocol included an initial denaturation at 95 °C for 10 min and following 40 cycles at 95 °C for 15 s, 58 °C for 30 s, and 72 °C for 60 s. All reactions were normalized to GAPDH. The specific primers for target genes were described in **Table 1**.

Histology

Mice were sacrificed under general anesthesia and intracardiacally perused with 10 ml 4% paraformaldehyde (PFA) at designed time postinoculation. The tympanic bullae were subsequently dissected, fixed overnight in 4% PFA and decalcified for 4 wk in 10% EDTA. After that, they were embedded in paraffin, sectioned at 7 μm, stained with hemotoxylin and eosin and digitally recorded with Nikon ECLIPSE 80i. The thickness of ME mucosa was analyzed with NIS-Elements BR 4.10.00 software by two pathologists in a blind manner.

Cell Quantification and Bacterial Load Determination

Mice were sacrificed and intracardiacally perused with 10 ml sterile PBS. The tympanic bullae were harvested and spilt into dorsal and ventral halves as described above. The exposed ME space was lavaged three times with 40 μl sterile PBS containing 5% fetal calf serum and total ME lavage fluid (MELF, ~120 μl) was collected. For enumeration of pneumococcal numbers, 10 μl MELF was serially diluted (10-fold) in sterile PBS and 10 μl samples of those dilutions was plated on Columbia sheep blood agar plates. The limit of detection was 120 CFU ($2.08Log_{10}$) per ME. When no colonies were detected, the number of *Spn* was assumed to be slightly under our limit of detection ($2.0Log_{10}$ bacteria in the ME). Another 10 μl MELF was added to 190 μl 1% acetic acid solution for total cell quantification based on standard morphological criteria using a blood cell counting plate. Residual MELF was centrifuged at 500 *g* for 10 min and supernatant for cytokine measurement was collected and stored at −70 °C until use.

ELISA

TNF-α, IL-6, IL-1β, and IL-17A in the MELF of WT and $TLR2^{-/-}$ mice at 1 and 7 d after *Spn* inoculation were determined with commercially available ELISA kits from R&D systems (Quantikine; Minneapolis) according to the manufacturer's instructions.

Flow Cytometry

The MELF of five mice from each group at 1 and 3 d after *Spn* inoculation were pooled, centrifuged at 500 *g*. The cell pellets were treated with RBC lysis buffer (Biolegend, San Diego, CA) and nonspecific binding was blocked with Mouse BD Fc Block in stain buffer (BD Pharmingen, Franklin Lakes, NJ). A cocktail of fluorophore-conjugated rat anti-mouse cell surface antibodies included APC-CD45 (BD Pharmingen), PE-Cy5-F4/80 (eBioscience, San Diego, CA), FITC-Ly6G (BD Pharmingen), PE-CD11b (BD Pharmingen), and their isotype antibodies were added for 45 min on the ice. After that, the cells were washed three times and resuspended in stain buffer prior to FACS analysis on a BD FACS Calibur flow cytometer (BD Biosciences, San Jose, CA).

Immunofluorescence

For TLR2 expression, the ME paraffin sections were deparaffinized, rehydrated, and incubated with 0.05% trypsin solution (Invitrogen, Carlsbad, CA) for 20 min at 37 °C to unmask antigens. After being washed in PBS, the sections were blocked with 5% normal donkey serum in PBS for 2 h at room temperature, and then incubated with rabbit anti-mouse TLR2 polyclonal antibody (1:200; Merck Millipore, Kenilworth, NJ) overnight at 4 °C. After the sections were further washed in PBS, a Alexa Fluor 594-conjugated donkey anti-rabbit IgG (1:800; Jackson ImmunoResearch, West Grove, PA) was added for 1 h at room temperature. For pneumococcal clearance, MELF was pooled from at least four mice, 100 μl of that was spun onto slides at 700 rpm for 5 min, desiccated for 15 min. After fixed in 2% PFA for 10 min, the cytospin preparations were blocked with 5% normal donkey serum, and then incubated with rabbit anti-pneumococcal polysaccharide polyclonal antibody (1:1,000; Staten Serum Institute, Denmark) as well as goat anti-mouse neutrophil elastase polyclonal antibody (1:200; Santa Cruz Biotechnology, Dallas, TX). Secondary antibodies were Alexa Fluor 488-conjugated donkey anti-rabbit IgG and Alexa Fluor 594-conjugated donkey anti-goat IgG (both1:800; Jackson ImmunoResearch). The slides were washed in PBS and counterstained with DAPI (1:1000; Invitrogen). Immunoflurescence images were collected using Nikon ECLIPSE 80i.

Statistical Analyses

All statistical analysis was performed using GraphPad prism software version 5.01 for Windows (GraphPad, La Jolla, CA). For analysis of CFU data between WT and $TLR2^{-/-}$ group, Mann-Whitney *U*-test was performed. For analysis of all other data, unpaired *t*-test was performed. $P < 0.05$ was considered statistically significant.

STATEMENT OF FINANCIAL SUPPORT

This research was supported by National Natural Science Foundation grants of China (No. csfc81373151), Scientific and Technological Research Program of Chongqing Municipal Education Commission grants of China (No. KJ130313), and Natural Science Foundation Project of CQCSTC (No. cstc2012jjA10014).

Disclosure: The authors state that they have no conflicts of interest.

REFERENCES

1. Vergison A, Dagan R, Arguedas A, et al. Otitis media and its consequences: beyond the earache. Lancet Infect Dis 2010;10:195–203.
2. Teele DW, Klein JO, Rosner B. Epidemiology of otitis media during the first seven years of life in children in greater Boston: a prospective, cohort study. J Infect Dis 1989;160:83–94.
3. Rovers MM, Schilder AG, Zielhuis GA, Rosenfeld RM. Otitis media. Lancet 2004;363:465–73.
4. Leichtle A, Lai Y, Wollenberg B, Wasserman SI, Ryan AF. Innate signaling in otitis media: pathogenesis and recovery. Curr Allergy Asthma Rep 2011;11:78–84.
5. Pichichero ME. Recurrent and persistent otitis media. Pediatr Infect Dis J 2000;19:911–6.
6. Ding Y, Geng Q, Tao Y, et al. Etiology and epidemiology of children with acute otitis media and spontaneous otorrhea in Suzhou, China. Pediatr Infect Dis J 2015;34:e102–6.
7. Dagan R, Leibovitz E, Greenberg D, Bakaletz L, Givon-Lavi N. Mixed pneumococcal-nontypeable Haemophilus influenzae otitis media is a distinct clinical entity with unique epidemiologic characteristics and pneumococcal serotype distribution. J Infect Dis 2013;208:1152–60.
8. Lieberthal AS, Carroll AE, Chonmaitree T, et al. The diagnosis and management of acute otitis media. Pediatrics 2013;131:e964–99.
9. Goossens H, Ferech M, Vander Stichele R, Elseviers M; ESAC Project Group. Outpatient antibiotic use in Europe and association with resistance: a cross-national database study. Lancet 2005;365:579–87.
10. Hotomi M, Billal DS, Kamide Y, et al.; Advanced Treatment for Otitis Media Study Group (ATOMS). Serotype distribution and penicillin resistance of Streptococcus pneumoniae isolates from middle ear fluids of pediatric patients with acute otitis media in Japan. J Clin Microbiol 2008;46:3808–10.
11. Pichichero ME, Casey JR. Emergence of a multiresistant serotype 19A pneumococcal strain not included in the 7-valent conjugate vaccine as an otopathogen in children. JAMA 2007;298:1772–8.
12. Medzhitov R. Recognition of microorganisms and activation of the immune response. Nature 2007;449:819–26.
13. Takeda K, Kaisho T, Akira S. Toll-like receptors. Annu Rev Immunol 2003;21:335–76.

14. Ku CL, von Bernuth H, Picard C, et al. Selective predisposition to bacterial infections in IRAK-4-deficient children: IRAK-4-dependent TLRs are otherwise redundant in protective immunity. J Exp Med 2007;204:2407–22.
15. Picard C, Puel A, Bonnet M, et al. Pyogenic bacterial infections in humans with IRAK-4 deficiency. Science 2003;299:2076–9.
16. von Bernuth H, Picard C, Jin Z, et al. Pyogenic bacterial infections in humans with MyD88 deficiency. Science 2008;321:691–6.
17. Albiger B, Sandgren A, Katsuragi H, et al. Myeloid differentiation factor 88-dependent signalling controls bacterial growth during colonization and systemic pneumococcal disease in mice. Cell Microbiol 2005;7:1603–15.
18. Koedel U, Rupprecht T, Angele B, et al. MyD88 is required for mounting a robust host immune response to Streptococcus pneumoniae in the CNS. Brain 2004;127(Pt 6):1437–45.
19. Schröder NW, Morath S, Alexander C, et al. Lipoteichoic acid (LTA) of Streptococcus pneumoniae and Staphylococcus aureus activates immune cells via Toll-like receptor (TLR)-2, lipopolysaccharide-binding protein (LBP), and CD14, whereas TLR-4 and MD-2 are not involved. J Biol Chem 2003;278:15587–94.
20. Letiembre M, Echchannaoui H, Bachmann P, et al. Toll-like receptor 2 deficiency delays pneumococcal phagocytosis and impairs oxidative killing by granulocytes. Infect Immun 2005;73:8397–401.
21. Knapp S, Wieland CW, van 't Veer C, et al. Toll-like receptor 2 plays a role in the early inflammatory response to murine pneumococcal pneumonia but does not contribute to antibacterial defense. J Immunol 2004;172:3132–8.
22. Echchannaoui H, Frei K, Schnell C, Leib SL, Zimmerli W, Landmann R. Toll-like receptor 2-deficient mice are highly susceptible to Streptococcus pneumoniae meningitis because of reduced bacterial clearing and enhanced inflammation. J Infect Dis 2002;186:798–806.
23. Koppe U, Suttorp N, Opitz B. Recognition of Streptococcus pneumoniae by the innate immune system. Cell Microbiol 2012;14:460–6.
24. Komori M, Nakamura Y, Ping J, et al. Pneumococcal peptidoglycan-polysaccharides regulate Toll-like receptor 2 in the mouse middle ear epithelial cells. Pediatr Res 2011;69:101–5.
25. Kaur R, Casey J, Pichichero M. Cytokine, chemokine, and Toll-like receptor expression in middle ear fluids of children with acute otitis media. Laryngoscope 2015;125:E39–44.
26. Nokso-Koivisto J, Chonmaitree T, Jennings K, Matalon R, Block S, Patel JA. Polymorphisms of immunity genes and susceptibility to otitis media in children. PLoS One 2014;9:e93930.
27. Mittal R, Robalino G, Gerring R, et al. Immunity genes and susceptibility to otitis media: a comprehensive review. J Genet Genomics 2014;41:567–81.
28. Han F, Yu H, Tian C, et al. Role for Toll-like receptor 2 in the immune response to Streptococcus pneumoniae infection in mouse otitis media. Infect Immun 2009;77:3100–8.
29. Shouval DS, Greenberg D, Givon-Lavi N, Porat N, Dagan R. Site-specific disease potential of individual Streptococcus pneumoniae serotypes in pediatric invasive disease, acute otitis media and acute conjunctivitis. Pediatr Infect Dis J 2006;25:602–7.
30. Ryan AF, Ebmeyer J, Furukawa M, et al. Mouse models of induced otitis media. Brain Res 2006;1091:3–8.
31. Albiger B, Dahlberg S, Sandgren A, et al. Toll-like receptor 9 acts at an early stage in host defence against pneumococcal infection. Cell Microbiol 2007;9:633–44.
32. Davis KM, Nakamura S, Weiser JN. Nod2 sensing of lysozyme-digested peptidoglycan promotes macrophage recruitment and clearance of S. pneumoniae colonization in mice. J Clin Invest 2011;121:3666–76.
33. Wang W, Zhou A, Zhang X, et al. Interleukin 17A promotes pneumococcal clearance by recruiting neutrophils and inducing apoptosis through a p38 mitogen-activated protein kinase-dependent mechanism in acute otitis media. Infect Immun 2014;82:2368–77.
34. Zhang Z, Clarke TB, Weiser JN. Cellular effectors mediating Th17-dependent clearance of pneumococcal colonization in mice. J Clin Invest 2009;119:1899–909.
35. Murray PJ, Wynn TA. Protective and pathogenic functions of macrophage subsets. Nat Rev Immunol 2011;11:723–37.
36. Erwig LP, Henson PM. Clearance of apoptotic cells by phagocytes. Cell Death Differ 2008;15:243–50.
37. Geissmann F, Manz MG, Jung S, Sieweke MH, Merad M, Ley K. Development of monocytes, macrophages, and dendritic cells. Science 2010;327:656–61.
38. Serbina NV, Jia T, Hohl TM, Pamer EG. Monocyte-mediated defense against microbial pathogens. Annu Rev Immunol 2008;26:421–52.
39. Melhus A, Ryan AF. A mouse model for acute otitis media. APMIS 2003;111:989–94.
40. Huang Y, Jin C, Xiang Y, et al. [A mouse model for acute otitis media via transbullar injection]. Zhonghua Er Bi Yan Hou Tou Jing Wai Ke Za Zhi 2015;50:318–23.